

EPJ E

Soft Matter and
Biological Physics

EPJ.org
your physics journal

Eur. Phys. J. E (2011) **34**: 48

DOI: 10.1140/epje/i2011-11048-1

Quantitative investigation of the two-state picture for water in the normal liquid and the supercooled regime

S.R. Accordino, J.A. Rodriguez Fris, F. Sciortino and G.A. Appignanesi



Società
Italiana
di Fisica



Springer

Quantitative investigation of the two-state picture for water in the normal liquid and the supercooled regime

S.R. Accordino¹, J.A. Rodriguez Fris^{1,a}, F. Sciortino², and G.A. Appignanesi¹

¹ Sección Físicoquímica - INQUISUR and Departamento de Química, Universidad Nacional del Sur, Avenida Alem 1253, 8000-Bahía Blanca, Argentina

² Dipartimento di Fisica and CNR-ISC, Università di Roma La Sapienza, Piazzale A. Moro 2, 00185 Roma, Italy

Received 21 December 2010 and Received in final form 19 March 2011

Published online: 16 May 2011 – © EDP Sciences / Società Italiana di Fisica / Springer-Verlag 2011

Abstract. Several evidences have helped to establish the two-state nature of liquid water. Thus, within the normal liquid and supercooled regimes water has been shown to consist of a mixture of well-structured, low-density molecules and unstructured, high-density ones. However, quantitative analyses have faced the burden of unambiguously determining both the presence and the fraction of each kind of water “species”. A recent approach by combining a local structure index with potential-energy minimisations allows us to overcome this difficulty. Thus, in this work we extend such study and employ it to quantitatively determine the fraction of structured molecules as a function of temperature for different densities. This enables us to validate predictions of two-state models.

1 Introduction

The comprehension of the structure and behaviour of water is paramount for different fields ranging from condensed matter and materials science to biology [1–12]. Liquid water presents several anomalies which become more conspicuous as it is supercooled below its melting temperature [8–11]. These anomalies have been tentatively associated to the presence of two competing preferential local structures identified with molecules characterised by high- or low-local density [9, 13–20], in a picture inspired by the existence of at least two different forms of amorphous glass states, namely low-density amorphous ice LDA and (very) high-density amorphous ice (V)HDA [21–24]. Several indicators [25–28, 13, 14] have been proposed to identify structured and unstructured molecules with partial success until recently we have introduced a combined approach (by using a local structural index together with minimisations of potential energy) which is able to quantify these two kinds of “species” [20]. We have also found that the inter-conversion between such kinds of molecules is at the heart of the dynamical events responsible for the structural (or α) relaxation [20, 29, 30] and have found a causal link between structure and dynamics [31, 32]. In the present work we shall study the robustness of the local structure index and the differences between structured and unstructured molecules in terms of the geometrical quality of their hydrogen bonds. We shall also perform a quantitative study of the fraction of structured water molecules as a func-

tion of temperature for different densities in order to test predictions of two-state models [17–19].

2 Methods: Detecting structured and unstructured molecules

For the sake of clarity, in this section we describe the method to determine structured and unstructured molecules [20]. We study, by means of molecular dynamics simulations, a system of 216 water molecules. These molecules interact via the Simple Point Charge (Extended) potential (SPC/E) [33] in a cubic box by using periodic boundary conditions and long-range interactions have been modelled via reaction field. We have studied systems at density 0.9, 0.95, 1.0 and 1.1 g/mL, in the T range from 320 K to 210 K. At the lowest T and ρ we simulated a trajectory of 300 ns. At this T and ρ the α -relaxation time, defined as the time at which the mean-squared displacement reaches the value 8 \AA^2 (the square of the most probable distance between two first-neighbour molecules), is 10 ns.

To study the local structure of water molecules on a quantitative basis, we use the indicator, proposed by Shiratani and Sasai [13, 14], which associates a local structure index (LSI) to each molecule to quantify the degree of local order. The key observation is the existence of certain molecules which show an unoccupied gap between 3.2 Å and 3.8 Å in their radial neighbour distribution for certain periods of time. Such low-density molecules

^a e-mail: rodriguezfris@plapiqui.edu.ar

are well structured and coordinated in a highly tetrahedral manner with other four water molecules. Occupancy of such gap increases the local density and distorts the tetrahedral order of the central molecule. Shiratani and Sasai [13,14] defined $LSI = I(i, t)$ for molecule i at time t . For each molecule i one orders the rest of the molecules depending on the radial distance r_j between the oxygen of the molecule i and the oxygen of molecule j : $r_1 < r_2 < r_j < r_{j+1} < \dots < r_{n(i,t)} < r_{n(i,t)+1}$, $n(i, t)$ is chosen so that $r_{n(i,t)} < r_{th} = 3.7 \text{ \AA} < r_{n(i,t)+1}$. Then, $I(i, t)$ is defined as [13,14]

$$I(i, t) = \frac{1}{n(i, t)} \sum_{j=1}^{n(i, t)} [\Delta(j; i, t) - \bar{\Delta}(i, t)]^2,$$

where $\Delta(j; i, t) = r_{j+1} - r_j$ and $\bar{\Delta}(i, t)$ is the average over all molecules of $\Delta(j; i, t)$. Thus, $I(i, t)$ expresses the inhomogeneity in the radial distribution within the sphere of radius around 3.7 \AA . A high value of $I(i, t)$ implies that molecule i at time t is characterised by a tetrahedral local order and a low-local density, while on the contrary, values of $I(i, t) \sim 0$ indicate a molecule with defective tetrahedral order and high-local density. Differently from refs. [13,14] we calculate such index in the inherent structures IS (minimising the potential energy of the corresponding instantaneous structure) to filter out the randomising effect introduced by the thermal vibrations [34], effectively removing the fluctuations present in the real trajectory which hamper the possibility of properly identifying the local structure.

Figure 1a shows the distribution of $I(i, t)$ in the range $210 \text{ K} \leq T \leq 320 \text{ K}$ for density $\rho = 1.0 \text{ g/mL}$. Direct inspection of such figure shows that for all studied temperatures the distribution —evaluated in the IS— is clearly bimodal. The left peak (whose amplitude decreases as T decreases) is indicative of unstructured (high-density) water molecules while the right peak (whose amplitude increases as T decreases) marks the presence of highly structured (low-density) molecules. It is important to notice that the position of the minimum (abscissa: $I_{\min} \sim 0.14 \text{ \AA}^2$) that separates the two peaks is invariant for all studied temperatures (a kind of “isosbestic point”), a strong indication of the existence of two populations with well-characterised local structures in dynamical equilibrium and whose relative concentration changes with T . This finding clearly supports a picture of supercooled water consisting of a mixture of molecules in two structural states, the fraction of structured molecules increasing as T is lowered. We also note that other indicators of local structure (which like the LSI have indeed provided first evidence for such a description), namely, the orientational order parameter q [25,26], the tetrahedrity parameter θ [27,28] or the total energy of the molecule [35], do not produce such clear bimodal distributions with a deep T -invariant minimum, not even at the IS level (only q and θ exhibit for some limited cases a very slight two-peak shape [26,28] but the use of the ISs does not improve the bimodality, as we have shown in [20]). For comparison, in fig. 1b we show the same

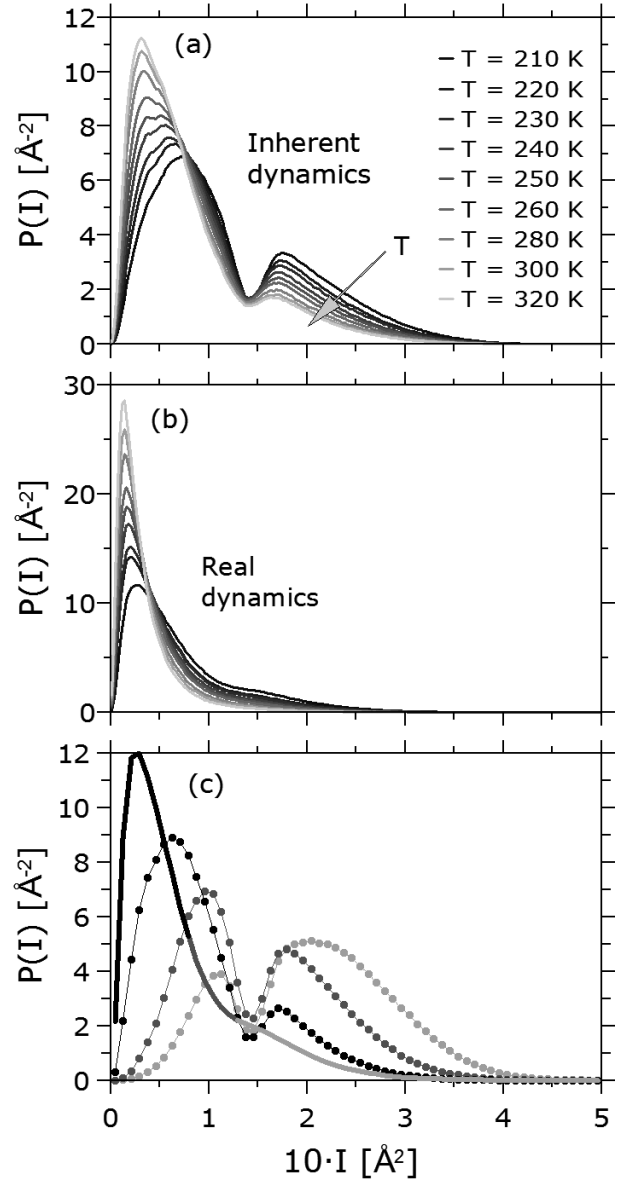


Fig. 1. Probability density $P(I)$ of finding a molecule with local structure index I , for density $\rho = 1.0 \text{ g/mL}$. For a range of temperatures within the normal and supercooled liquid regimes, data for: (a) inherent dynamics, (b) real dynamics. Legend in (a) applies also for (b). (c) For $T = 210 \text{ K}$ we consider the set of molecules that in (b) has $0 \leq I/\text{\AA}^2 < 0.075$ (black thick curve), the set of molecules that in (b) has $0.075 \leq I/\text{\AA}^2 < 0.12$ (dark-grey thick curve) and the set of molecules that in (b) has $0.12 \leq I/\text{\AA}^2 < \infty$ (light-grey thick curve). Then, for each set of molecules we plot the corresponding $P(I)$ (symbols, same greyscale) but taking the I of the molecules in the inherent dynamics.

picture but calculated at the instantaneous or real configurations (that is, without the minimisation procedure).

Assuming that (for any given T) the distribution of the LSI (fig. 1a) is the result of the contributions of two different distributions (one for structured and other for unstructured molecules) and given the pronounced slopes

of the curve at both sides of $I_{\min} \sim 0.14 \text{ \AA}^2$, the overlapping between the two distributions would be quite small. Thus, the area beneath the second peak of fig. 1a represents an estimate for the fraction of structured molecules present in the sample. This fraction ξ is calculated integrating the curve $P(I)$ between I_{\min} and ∞ .

We wish to note that Shiratani and Sasai [13] have noted the existence of transition and unstable configurations together with certain discrepancies between (a direct interpretation of) the information given by the real and the inherent dynamics. They noticed that at the times when a molecule is in transition configurations between both kind of states (structured and unstructured) it tends to alternate between moderately high and moderately low LSI values at the real dynamics. We expect that in our case the minimisation procedure would lead these configurations to one of the two states depending on their proximity to (the crossing point between) each of them at the corresponding time. The minimisation procedure, as evident from the LSI distribution of fig. 1a, brings the actual configuration to the local minimum at the bottom of its basin of attraction, and thus, only the structured and the unstructured states are stable (low-energy or high-energy minima, respectively, but nevertheless local minima) while transition configurations are not stable. Thus, the existence of transition configurations is not a problem for the two-state description. To better study this point we (arbitrarily) divided the LSI distribution for the real dynamics at $T = 210 \text{ K}$ in three classes: molecules with $I/\text{\AA}^2 < 0.075$, $0.075 < I/\text{\AA}^2 < 0.12$ and $I/\text{\AA}^2 > 0.12$. Thus, we can speak of molecules with low, medium and high LSI values, respectively. Then for the low-LSI molecules we considered the corresponding inherent configurations and calculated their LSI distribution. In the same way we calculated the LSI distributions at the inherent dynamics for the medium- and high-LSI molecules, as discriminated at the real dynamics. The results can be seen in fig. 1c. The solid thick line corresponds to the LSI distribution for the real dynamics. The curves with circles show the LSI distributions at the inherent level of the three kinds of molecules. The one with black circles represents the case of the low-LSI molecules, the one with dark-grey circles corresponds to the medium-LSI molecules and the curve with light-grey circles is for high-LSI molecules. We can see that both the real and the inherent calculations can adequately distinguish the great majority of the well-structured and of the unstructured molecules. For example, 79% of the low-LSI molecules (so classified at the real configurations) fall before the minimum I_{\min} of the inherent LSI distribution, that is, they lie within the peak for unstructured molecules. In turn, 76% of the high-LSI molecules fall within the structured peak at the inherent distribution. Finally, we can see that the molecules with medium LSI values are equally partitioned between the structured and unstructured states (50% of the area at both sides of I_{\min}). Transition configurations mostly correspond to this last class of molecules and thus represent a minority part of all the configurations. Thus, notwithstanding the dynamical importance of transition configurations,

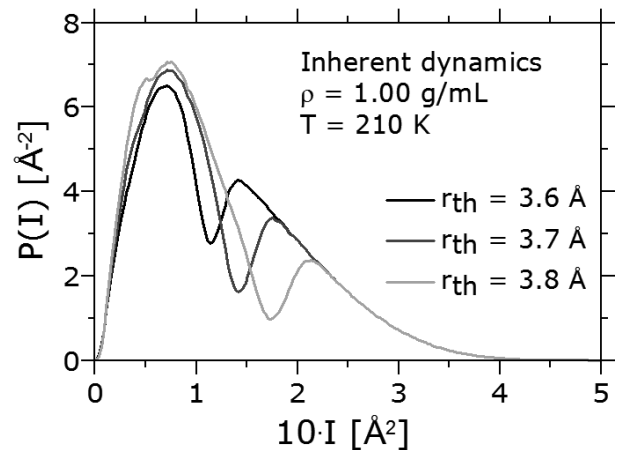


Fig. 2. $P(I)$ for different threshold radii r_{th} in the calculation of the local structure index I for density $\rho = 1.0 \text{ g/mL}$ and $T = 210 \text{ K}$: $r_{\text{th}} = 3.6 \text{ \AA}$ (black), $r_{\text{th}} = 3.7 \text{ \AA}$ (dark grey, the classic value) and $r_{\text{th}} = 3.8 \text{ \AA}$ (light grey).

urations, we can see that both the well-structured and unstructured molecules are nicely captured by both the real and inherent LSI distributions and that the two-state picture remains as a good description. Transition configurations that occur at any given time are not stable with respect to minimisation and thus, at the IS level they contribute to both states depending on their proximity to each of them at such time.

Finally, we wish to note that perfect cubic ice gives a value of LSI of 0.43 \AA^2 , while perfect hexagonal ice (ice I h) gives 0.54 \AA^2 . We note that these cases correspond to $T = 0$, that is, structures free from thermal fluctuations. Thus, we calculated the mean LSI value for hexagonal ice at $T = 100 \text{ K}$ and $T = 200 \text{ K}$. The values we obtained are respectively 0.20 \AA^2 and 0.15 \AA^2 . Such values are within the peak for structured molecules in fig. 1a for supercooled water.

3 Results and discussion

3.1 Robustness of the local structure index

Given the evident usefulness of the local structure index indicator, a natural question that emerges regards its robustness. This index uses a rather arbitrary threshold radius of $r_{\text{th}} = 3.7 \text{ \AA}$ (even when carefully chosen from the position of the minimum between the first two peaks in the radial distribution function) to determine the neighbours to be considered in order to perform calculation. Thus, we are interested in determining whether the results are still valid for moderate changes in such threshold. In fig. 2 we show the distributions of the local structure index $P(I)$ at unitary density and $T = 210 \text{ K}$ but when the index is calculated with thresholds of $r_{\text{th}} = 3.6 \text{ \AA}$ and 3.8 \AA . We can see that in both cases, the distributions are still clearly bimodal, a fact that also holds for all the other temperatures considered (data not shown). However, now the position of the minimum I_{\min} varies. This means that the estimation

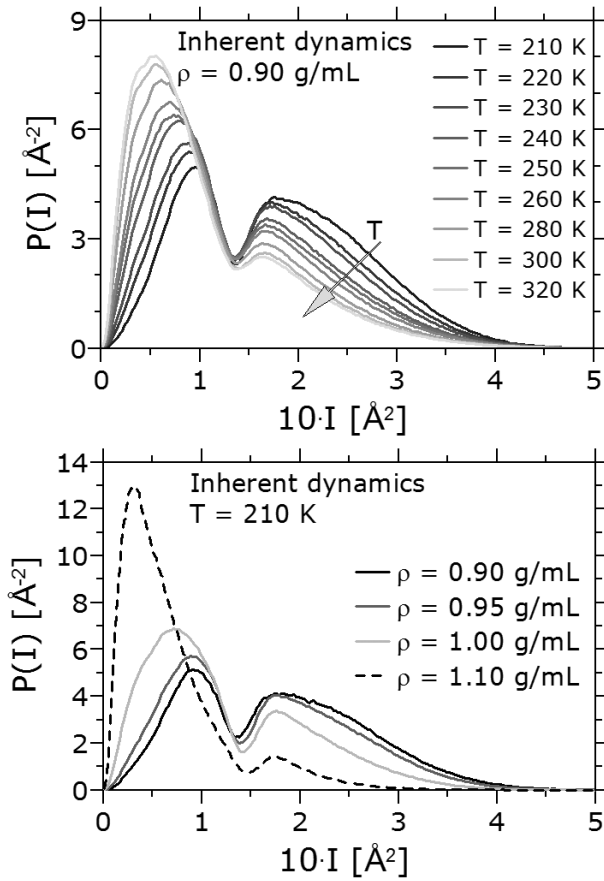


Fig. 3. Top: $P(I)$ for the nine studied temperatures T and density $\rho = 0.9$ g/mL. Bottom: $P(I)$ for the four studied densities and $T = 210$ K.

of the fraction of structured or unstructured molecules depends on this threshold value. Nevertheless, later on we shall see that the functional dependence with temperature of the fraction of structured molecules ξ does not depend on it.

3.2 Changes of water structure with density

Another point of interest is whether the bimodality in $P(I)$ emerges only in the case of unitary density or if it still holds for other density values. Thus, we performed the analysis for all studied ρ and T . In fig. 3 we present some results: top fig. 3 shows the analysis performed for constant $\rho = 0.90$ g/mL and all studied T . Although not shown, a clear bimodality is present for other ρ and T . Bottom fig. 3 shows data for fixed $T = 210$ K and variable ρ . For densities lower than unity, it is expected that for any fixed temperature the fraction of structured molecules would increase as the low local density state would be stabilised, while the opposite should hold for densities higher than unity. Here we show that while this is in fact the case, the bimodality is not changed but the populations of the two states are modified. Moreover, we can learn that the value of I_{\min} is rather unaltered for fixed ρ .

3.3 Quality of hydrogen bonding parameters for structured and unstructured molecules

Given the fact that we can discriminate between structured and unstructured water molecules it would be interesting to quantify the quality of the hydrogen bonding interactions in which molecules of both types are engaged. Typically, each water molecule i tends to be surrounded by four first neighbours j to which it binds via hydrogen bonds. We must take into account that we are employing the inherent dynamics technique that refines the structure (the configurations represent local-potential-energy minima) and thus, the local geometries (hydrogen bond distances and angles) would be much improved as compared with instantaneous configurations. However, the local structure index I clearly discriminates between structured and unstructured molecules in the inherent configurations and thus, we expect differences in the local geometrical parameters for both kinds of molecules. To this end we calculated for each density and temperature the distributions of the hydrogen bond (HB) parameters for structured and unstructured molecules. For the mean HB distance, $\langle r_{\text{HB}} \rangle$, we take the distance between the oxygen of a water molecule i and the oxygen of a water molecule j . In turn, if a molecule i is hydrogen-bonded via one of its hydrogen atoms to a molecule j , we consider the HB lowest angle A to be that formed between the lines joining O_i with H_i and H_i with O_j (a perfect HB would present a 0° value). Given the fact that the minimisation procedure improves the local geometries, for the distance and angle distributions we considered that each water molecule is hydrogen-bonded to its first four neighbours (in fact, the minimisation produces well-developed HBs, as indicated by the resulting distance and angle distributions we obtain). In fig. 4 we plot $\langle r_{\text{HB}} \rangle$ for structured (filled symbols, top figure) and unstructured (open symbols, bottom figure) molecules (the ones to the right or to the left of the I_{\min} value of the corresponding $P(I)$ distribution, respectively) as a function of T for the four studied ρ . As expected, $\langle r_{\text{HB}} \rangle$ is lower for higher densities. This value is clearly T -dependent and decreases as T diminishes since HBs geometries improve with cooling. If we focus on the curves for unitary density we can see that the HBs at any fixed T are much shorter (thus, better, stronger HBs) for the structured than for the unstructured molecules. While this is an expected result, what is notable is the great difference between them. For example at $\rho = 1.0$ g/mL, $\langle r_{\text{HB}} \rangle$ for a structured molecule at $T = 320$ K is comparable to that for an unstructured molecule at a temperature as low as $T = 230$ K, well within the supercooled regime. This trend is also qualitatively valid for other ρ .

In fig. 5 we show the standard deviation σ_A from the mean value of the HB lowest angle (A) distribution for structured (filled symbols) and unstructured (open symbols) molecules as a function of T for the four studied densities (deviations from 0° make the HB weaker). σ_A is defined as $\{n^{-1} \sum_{i=1}^n [A_i - \langle A \rangle]^2\}^{1/2}$, where n is the number of HBs, A_i is the angle in the i -th HB and $\langle A \rangle$ is $n^{-1} \sum_{i=1}^n A_i$. As expected, the structured molecules

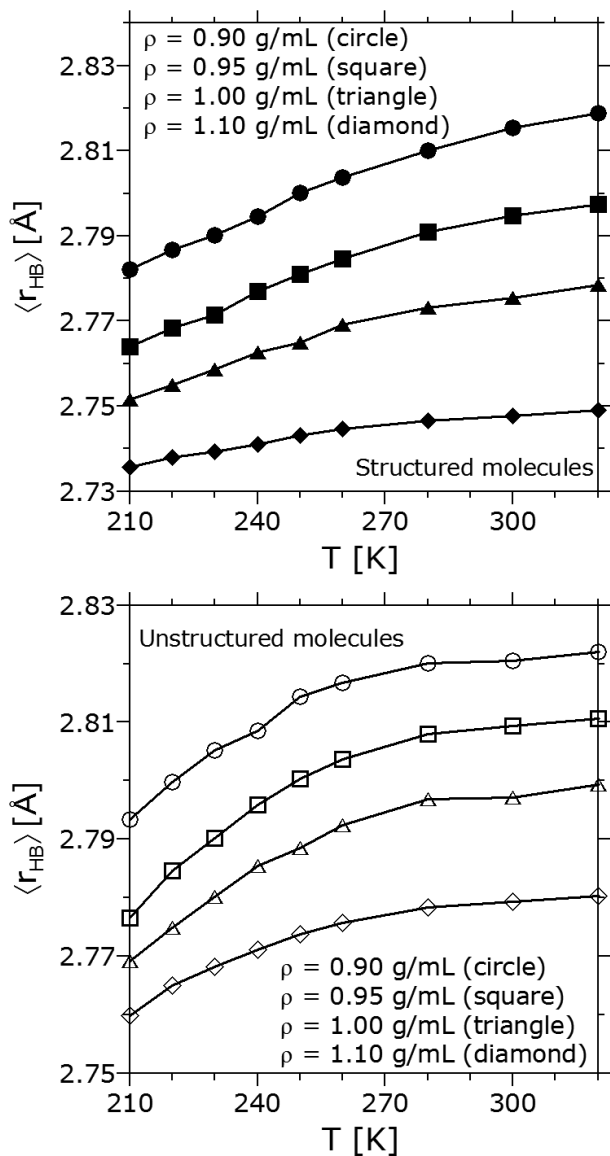


Fig. 4. Mean hydrogen bond distance, $\langle r_{\text{HB}} \rangle$, for structured (filled symbols, top figure) and unstructured (open symbols, bottom figure) molecules for the four studied densities ρ , as a function of temperature.

deviate less than the unstructured ones. All results are consistent with the ones obtained with the mean HB distance data. For example for unitary density, σ_A for structured molecules at $T = 320$ K is comparable to that of the unstructured molecules at temperatures lower than 210 K.

3.4 Temperature dependence of the fraction of structured molecules. Testing two-state model predictions

In this section we shall quantify the fraction of structured water molecules at the different studied temperatures and densities. These data would be compared with the predictions of a two-state model [17–19]. Amongst the differ-

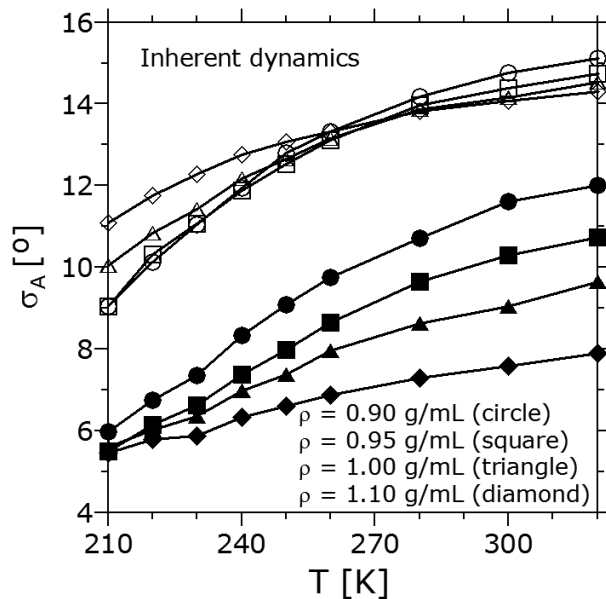


Fig. 5. Standard deviation, σ_A , in the HB-lowest-angle distribution for structured (filled symbols) and unstructured (open symbols) molecules for the four studied densities ρ , as a function of temperature.

ent two-state models of water that have been proposed it seems interesting to refer briefly to two different recent descriptions: The mixture model [36–40] and the two-order-parameter model [17–19]. While in the first case water is supposed to exist in one of two differently structured motifs (like for example LDA and HDA), the second one regards water as a mixture of a few structured locally favoured molecular arrangements and an unstructured liquid-like state that can have many different local configurations. Both models consider the existence of a structured state made of one (or few) locally well-arranged molecules. Thus, the main difference consists in the fact that the two-order-parameter model considers an unstructured state consisting of a set of many different configurations, which implies that it poses a large entropy, while the mixture model considers that such state is rather unique (and not necessarily unstructured but with a local structure different from the other state). The use of the real dynamics to calculate local structure indices, as has been done up to now, does not help much in this respect. This is so since as concerns the local structure index LSI, thermally induced distortions of a locally preferred structure can yield an outcome not easily distinguishable from that of a plethora of different configurations. Thus, our results based on inherent dynamics (where the randomising effect of thermal fluctuations is explicitly removed by conducting each configuration to its locally energetically preferred structure or local minimum of the basin of attraction where it belongs) can provide relevant evidence. First of all, from the shape of the peaks of fig. 1a and fig. 3 it seems that at all studied temperatures and densities the unstructured (and also the structured state) is not represented by a single unique configuration but rather by many different local configurations. Also interesting is the fact that the ab-

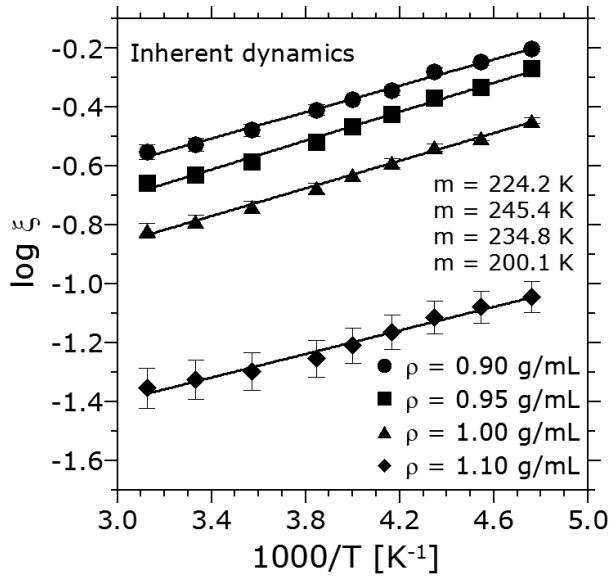


Fig. 6. Fraction of area ξ beneath the structured part of the LSI-distribution plot $P(I)$ against reciprocal absolute temperature for the four studied densities ρ . ξ is evaluated as $\int_{I_{\min}}^{\infty} P(I)dI$. Linear fits of the data are included, marked by the solid lines. Slopes m of the corresponding linear fits are shown, from top to bottom set, respectively: 224.2 K, 245.4 K, 234.8 K and 200.1 K. Error bars of $\pm 5\%$ of the corresponding value are also included.

scissa position of the maximum in the structured peak and of the minimum separating the two peaks (I_{\min}) are fairly temperature and density independent, while the abscissa position of the maximum in the unstructured peak moves significantly in the temperature range studied. Thus, these findings are in principle consistent with a structured state that entails the contribution of a few well-defined local configurations and an unstructured state representing a high-entropy state arising from many different configurations with no local structural preference.

Another prediction of the two-order-parameter model is that the fraction of the structured component (for low-fraction values) should be described by a Boltzmann factor (where the Boltzmann weight expresses the stabilisation due to the hydrogen bond energy of the locally favoured well-developed hydrogen bonds structure and the destabilisation, proportional to the pressure, stemming from the concurrent volume increase [17–19]). Thus, the fraction of structured molecules would display an exponential dependence on the reciprocal absolute temperature.

To test this prediction, for the different densities studied we calculated the fraction of structured molecules, ξ , by integrating the corresponding curve $P(I)$ between I_{\min} and ∞ . In fig. 6 we plot for each of the densities the curve for $\log \xi$ versus $1/T$. We can clearly see that the data can in all cases be well fitted by a linear dependence, as demanded by the two-order-parameter model.

Comparing the slopes m of the linear tendencies for densities 0.90, 0.95 and 1.00 g/mL, we see that they lie within 10%, although including the value for $\rho = 1.10$ g/mL the values lie within 20%. It is worth noting

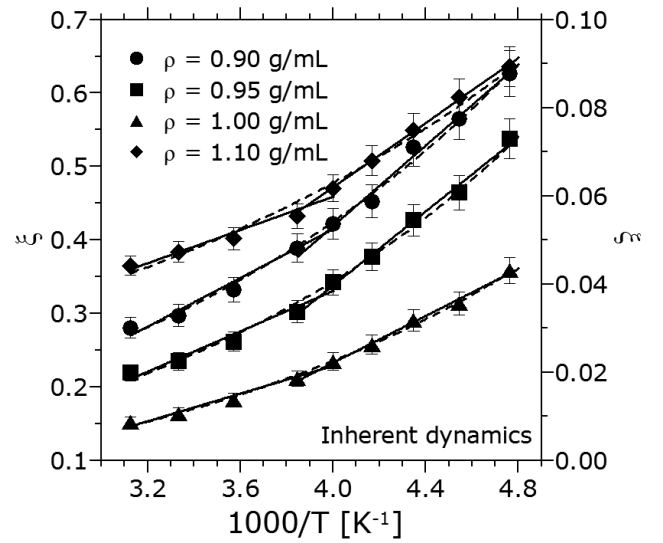


Fig. 7. Fraction of structured area ξ against reciprocal absolute temperature for four densities ρ . Error bars represent $\pm 5\%$. Left axis: $\rho \leq 1.00$ g/mL, right axis: $\rho = 1.10$ g/mL. An exponential fit of the corresponding data is included (dashed curves). For each of the four densities, two linear fits of the corresponding data are included (solid lines), one for low T and other for high T . For constant ρ these lines cross at $T \sim 250$ K.

that each fit lies within $\pm 5\%$ with respect of their respective data.

In fig. 7 we show the same data reported in fig. 6, but the data are now fitted with an exponential. Again, the two-state model prediction is consistent with the data. However, the data can also be well fitted by two linear tendencies (one for the high- and the other for the low- T regime) and each pair of lines for each of the four densities cross at $T \sim 250$ K.

We have previously shown in sect. 3.1 that moderate changes in the threshold radius value r_{th} to calculate the local structure index I do not affect the bimodality of the index distribution $P(I)$ (fig. 2) but that they shift the position of the minimum between the two maxima (that is, the value of I_{\min}). It would thus be worthwhile to study whether the above-mentioned temperature dependence of the fraction of structured molecules ξ is robust with respect to these changes in the threshold radius value. In fig. 8 we plot ξ against $1/T$ for density 1.0 g/mL and the three threshold values of r_{th} used for evaluating the index I . From the good linear fits we can learn that the functional dependence is the same in all cases.

4 Conclusions

In this work we have explored the robustness and validity (for different densities and temperatures) of a method to determine structured and unstructured water molecules and we have determined the (geometrical) quality of the local order of both kinds of molecules. Also, by determining the fraction of structured molecules (within the normal liquid and supercooled liquid regimes) we have

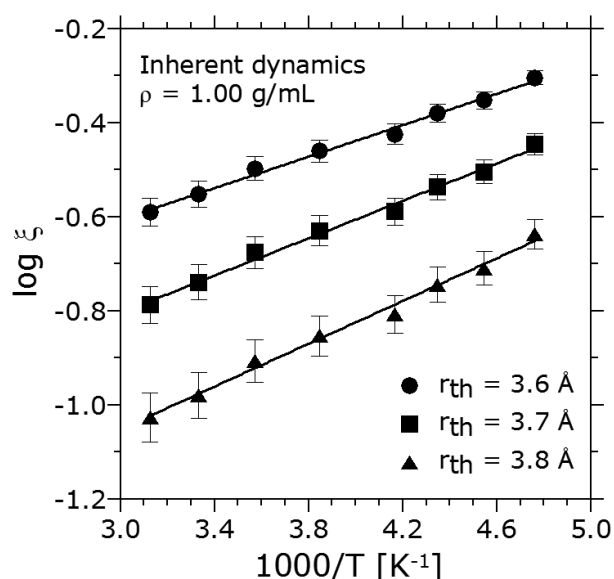


Fig. 8. ξ against $1/T$ for density 1.0 g/mL and three threshold values r_{th} for evaluating the local structure index I . Error bars of $\pm 5\%$ of the corresponding value are also included. A linear fit of each set of data is included (solid lines).

tested two-state model predictions. In particular, we have demonstrated that the fraction of structured molecules can indeed be described by a Boltzmann factor entailing the enthalpic and volumetric contributions involved in the local order development. It would be interesting in a future study to apply the methods discussed in this article to model potentials which show a clear liquid-liquid critical point [41,42], to assess if the LSI analysis, when applied to state points close to the critical one, can shed light on the relevant order parameter characterising the transition between the low-density and high-density liquid phases [43] and if the LSI analysis can help to trace a formal connection between the two-state fluctuations associated to the critical point and the two-state fluctuations observed in standard conditions.

FS acknowledges support from ERC-226207-PATCHY-COLLOIDS. Financial support from ANPCyT (PME 2006-1581), MinCyT and CONICET is also gratefully acknowledged. GAA and JARF are research fellows of CONICET. SRA thanks CONICET for a fellowship.

References

- D.M. Huang, D. Chandler, Proc. Natl. Acad. Sci. U.S.A. **97**, 8324 (2000).
- X. Huang, C.J. Margulis, B.J. Berne, Proc. Natl. Acad. Sci. U.S.A. **100**, 11953 (2003).
- A. Bizzarri, S. Cannistraro, J. Phys. Chem. B **106**, 6617 (2002).
- D. Vitkup, D. Ringe, G.A. Petsko, M. Karplus, Nat. Struct. Biol. **7**, 34 (2000).
- N. Choudhury, B. Montgomery Pettitt, J. Phys. Chem. B **109**, 6422 (2005).
- H.E. Stanley, P. Kumar, L. Xu, Z. Yan, M.G. Mazza, S.V. Buldyrev, S.-H. Chen, F. Mallamace, Physica A **386**, 729 (2007).
- N. Giovambattista, P.G. Debenedetti, C.F. Lopez, P.J. Rossky, Proc. Natl. Acad. Sci. U.S.A. **105**, 2274 (2008).
- P.G. Debenedetti, *Metastable Liquids* (Princeton University Press, Princeton, NJ, 1996).
- O. Mishima, H.E. Stanley, Nature **396**, 329 (1998).
- C.A. Angell, Chem. Rev. **102**, 2627 (2002).
- C.A. Angell, Annu. Rev. Phys. Chem. **55**, 559 (2004).
- D.C. Malaspina, E.P. Schulz, L.M. Alarcón, M.A. Frechero, G.A. Appignanesi, Eur. Phys. J. E **32**, 35 (2010).
- E. Shiratani, M. Sasai, J. Chem. Phys. **104**, 7671 (1996).
- E. Shiratani, M. Sasai, J. Chem. Phys. **108**, 3264 (1998).
- M. Sasai, Physica A **285**, 315 (2000).
- M. Sasai, J. Chem. Phys. **118**, 10651 (2003).
- H. Tanaka, Phys. Rev. Lett. **80**, 5750 (1998).
- H. Tanaka, Europhys. Lett. **50**, 340 (2000).
- H. Tanaka, J. Chem. Phys. **112**, 799 (2000).
- G.A. Appignanesi, J.A. Rodriguez Fris, F. Sciortino, Eur. Phys. J. E **29**, 305 (2009).
- O. Mishima, L.D. Calvert, E. Whalley, Nature **310**, 393 (1984).
- H.-G. Heide, Ultramicroscopy **14**, 271 (1984).
- T. Loerting, C. Salzmann, I. Kohl, E. Mayer, A. Hallbrucker, Phys. Chem. Chem. Phys. (Inc. Faraday Trans.) **3**, 5355 (2001).
- T. Loerting, N. Giovambattista, J. Phys.: Condens. Matter **18**, 919 (2006).
- P.-L. Chau, A.J. Hardwick, Mol. Phys. **93**, 511 (1998).
- J.R. Errington, P.G. Debenedetti, Nature **409**, 318 (2001).
- Yu.I. Naberukhin, V.P. Voloshin, N.N. Medvedev, Mol. Phys. **73**, 917 (1991).
- A. Oleinikova, I. Brovchenko, J. Phys.: Condens. Matter **18**, S2247 (2006).
- J.A. Rodriguez Fris, G.A. Appignanesi, E. La Nave, F. Sciortino, Phys. Rev. E **75**, 041501 (2007).
- G.A. Appignanesi, J.A. Rodriguez Fris, R.A. Montani, W. Kob, Phys. Rev. Lett. **96**, 057801 (2006).
- D.C. Malaspina, J.A. Rodriguez Fris, G.A. Appignanesi, F. Sciortino, EPL **88**, 16003 (2009).
- G.A. Appignanesi, J.A. Rodriguez Fris, M.A. Frechero, Phys. Rev. Lett. **96**, 237803 (2006).
- H.J.C. Berendsen, J.R. Grigera, T.P. Stroatsma, J. Phys. Chem. **91**, 6269 (1987).
- P.G. Debenedetti, F.H. Stillinger, Nature **410**, 259 (2001).
- F. Sciortino, A. Geiger, H.E. Stanley, J. Chem. Phys. **96**, 3857 (1992).
- C.H. Cho, S. Singh, G.W. Robinson, Phys. Rev. Lett. **76**, 1651 (1996).
- J. Urquidi, S. Singh, C.H. Cho, G.W. Robinson, Phys. Rev. Lett. **83**, 2348 (1999).
- E.G. Ponyatovsky, V.V. Sinitsyn, T.A. Pozdnyakova, JETP Lett. **60**, 360 (1994).
- E.G. Ponyatovsky, V.V. Sinitsyn, T.A. Pozdnyakova, J. Chem. Phys. **109**, 2413 (1998).
- E.G. Ponyatovsky, J. Phys.: Condens. Matter **15**, 6123 (2003).
- P.H. Poole, F. Sciortino, U. Essmann, H.E. Stanley, Nature **360**, 324 (1992).
- P.H. Poole, I. Saika-Voivod, F. Sciortino, J. Phys.: Condens. Matter **17**, L431 (2005).
- M.J. Cuthbertson, P.H. Poole, Phys. Rev. Lett. **106**, 115706 (2011).